



Research paper

A single-dose plasmid-launched live-attenuated Zika vaccine induces protective immunity



Jing Zou^a, Xuping Xie^a, Huanle Luo^b, Chao Shan^a, Antonio E. Muruato^{a,b}, Scott C. Weaver^{b,c,d,e,f}, Tian Wang^{b,d,g}, Pei-Yong Shi^{a,c,d,e,f,g,h,*}

^a Department of Biochemistry & Molecular Biology, University of Texas Medical Branch, Galveston, TX, USA

^b Department of Microbiology & Immunology, University of Texas Medical Branch, Galveston, TX, USA

^c Institute for Human Infections & Immunity, University of Texas Medical Branch, Galveston, TX, USA

^d Sealy Institute for Vaccine Sciences, University of Texas Medical Branch, Galveston, TX, USA

^e Institute for Translational Sciences, University of Texas Medical Branch, Galveston, TX, USA

^f Sealy Center for Structural Biology & Molecular Biophysics, University of Texas Medical Branch, Galveston, TX, USA

^g Department of Pathology, University of Texas Medical Branch, Galveston, TX, USA.

^h Department of Pharmacology & Toxicology, University of Texas Medical Branch, Galveston, TX, USA

ARTICLE INFO

Article history:

Received 10 August 2018

Received in revised form 29 August 2018

Accepted 29 August 2018

Available online 7 September 2018

Keywords:

Zika virus

DNA vaccine

live-attenuated vaccine

flavivirus

ABSTRACT

Background: Vaccines are the most effective means to fight and eradicate infectious diseases. Live-attenuated vaccines (LAV) usually have the advantages of single dose, rapid onset of immunity, and durable protection. DNA vaccines have the advantages of chemical stability, ease of production, and no cold chain requirement. The ability to combine the strengths of LAV and DNA vaccines may transform future vaccine development by eliminating cold chain and cell culture with the potential for adventitious agents.

Methods: A DNA-launched LAV was developed for ZIKV virus (ZIKV), a pathogen that recently caused a global public health emergency. The cDNA copy of a ZIKV LAV genome was engineered into a DNA plasmid. The DNA-LAV plasmid was delivered into mice using a clinically proven device TriGrid™ to launch the replication of LAV.

Findings: A single-dose immunization as low as 0.5 µg of DNA-LAV plasmid conferred 100% seroconversion in A129 mice. All seroconverted mice developed sterilizing immunity, as indicated by no detectable infectious viruses and no increase of neutralizing antibody titers after ZIKV challenge. The immunization also elicited robust T cell responses. In pregnant mice, the DNA-LAV vaccination fully protected against ZIKV-induced disease and maternal-to-fetal transmission. High levels of neutralizing activities were detected in fetal serum, indicating maternal-to-fetal humoral transfer. In male mice, a single-dose vaccination completely prevented testis infection, injury, and oligospermia.

Interpretation: The remarkable simplicity and potency of ZIKV DNA-LAV warrant further development of this vaccine candidate. The DNA-LAV approach may serve as a universal vaccine platform for other plus-sense RNA viruses.

Fund: National Institute of Health, Kleberg Foundation, Centers for Disease Control and Prevention, University of Texas Medical Branch.

© 2018 The Authors. Published by Elsevier B.V. This is an open access article under the CC BY-NC-ND license (<http://creativecommons.org/licenses/by-nc-nd/4.0/>).

1. Introduction

Zika virus (ZIKV) is a mosquito-borne member from the genus *Flavivirus* within the family *Flaviviridae*. Besides ZIKV, many flaviviruses are significant human pathogens that cause frequent outbreaks and epidemics around the world, including dengue (DENV), yellow fever

(YFV), West Nile (WNV), Japanese encephalitis (JEV), and tick-borne encephalitis virus (TBEV). Flaviviruses have a positive-sense, single-stranded RNA genome of about 11,000 nucleotides in length. The viral genome contains a 5' untranslated region (UTR), a long open-reading frame, and a 3' UTR. The single open-reading frame encodes three structural (capsid [C], precursor membrane [prM] and envelope [E]) and seven non-structural (NS1, NS2A, NS2B, NS3, NS4A, NS4B and NS5) proteins. The structural proteins, together with the genomic RNA, form viral particles. The nonstructural proteins participate in viral replication, virion assembly, and evasion of the host innate immune response [1].

* Corresponding author at: Department of Biochemistry & Molecular Biology, University of Texas Medical Branch, Galveston, TX, USA.
 E-mail address: peshi@utmb.edu (P.-Y. Shi).

Research in context

Enhancing vaccine performance with improved simplicity and immunity is critical, particularly when responding to epidemic emergencies. The ability to combine the advantages of different vaccine platforms could transform future vaccine development. Using Zika virus (ZIKV) as a model, we developed a DNA-launched live-attenuated vaccine (LAV) that combines the advantages of DNA vaccines (chemical stability, no cold chain, easy production, and low cost) and LAVs (single dose, quick immunity and durable protection). Remarkably, a single-dose vaccination as low as 0.5 µg of the DNA-LAV plasmid elicited 100% protective immunity within 14–21 days in A129 mice. The vaccination completely prevented ZIKV infection, *in utero* transmission during pregnancy, and male reproductive tract infections. Besides antibody response, the immunized mice also developed robust T cell responses. Compared with previous DNA-launched LAV studies, this study showed lower minimal plasmid dose (0.5 µg) required for 100% protection and, for the first time, that a DNA-launched LAV is able to elicit sterilizing immunity as well as robust T cell responses. The DNA-launched approach could serve as a universal platform to deliver LAVs for other positive-sense, single-stranded RNA viruses.

ZIKV was first identified from a sentinel rhesus macaque in the Ziika Forest of Uganda in 1947 [2]. Before 2007, ZIKV had silently circulated between primates and mosquitoes in the forests in Africa and Southeast Asia without causing detectable outbreaks or severe human diseases. Symptomatic ZIKV infection produces mild manifestations, such as fever, headaches, lethargy, conjunctivitis, rash, arthralgia, and myalgia [3]. However, from 2007 to 2016, ZIKV emerged explosively to cause a series of epidemics in Africa, Micronesia, the South Pacific, and the Americas, leading to >700,000 documented autochthonous human infections [4,5]. Importantly, during the recent epidemics, ZIKV caused the newly described devastating congenital Zika syndromes (CZS), including microcephaly, craniofacial disproportion, spasticity, ocular abnormalities, and miscarriage [6]. CZS was found in 6–11% of the fetuses from ZIKV-infected pregnant women [7]. In adults, Zika infection can cause Guillain-Barré syndrome (GBS; an autoimmune disease that leads to muscle weakness and paralysis) at an incidence of 1 in 4000–to-5000 infected adults [8]. From February to November of 2016, the World Health Organization (WHO) declared ZIKV-related CZS as a Public Health Emergency of International Concern [4].

In response to the ZIKV epidemics, intensive efforts have been made to develop countermeasures, including vaccines and antivirals, with vaccines showing great promise [9–11]. Three types of vaccines are being pursued: (i) Inactivated vaccine. Two doses of a formalin-inactivated ZIKV vaccine elicited protective levels of neutralizing antibodies in phase I clinical trials [12,13]. (ii) Subunit vaccine. Subunit vaccines express the viral prM-E proteins from DNA, mRNA, or viral vectors (including measles virus, vesicular stomatitis virus, adenovirus, and modified vaccinia virus) [14–19]. Three-dose immunizations of DNA subunit vaccines induced protective humoral and cellular immune responses in phase I clinical trials [20,21]. (iii) Live-attenuated vaccine (LAV). Both attenuation of wild-type (WT) ZIKV and chimeric flavivirus approaches have been pursued to develop LAVs. For the former, LAV candidates containing a 3'UTR deletion showed excellent safety and potency in mouse and non-human primate (NHP) models [22,23]. For the later approach, chimeric DENV-2 and JEV SA14-14-2 with swapped ZIKV prM-E genes were reported to protect mice and/or NHPs from ZIKV infection after a single-dose vaccination [24,25].

Different vaccine platforms have distinct features. Compared with LAVs, DNA vaccines are chemically stable and do not require a cold chain. However, traditional DNA vaccines expressing viral antigens

usually require multiple doses, and the immune responses observed in animal models have generally not been reproduced in humans [26]. In contrast, LAVs usually have the advantages of single dose, quick immunity, and durable protection. However, the manufacture and transport of LAVs require cell culture (or eggs) and a cold chain. The cold chain alone can account for 80% of the vaccine cost in warm climates where emerging viruses are typically endemic [27]. Thus, a DNA-launched LAV has the potential to combine the strengths and to eliminate the weaknesses of both vaccine platforms. These improvements are of practical importance and could transform future vaccine development. To achieve this goal, we have developed a single-dose DNA-launched LAV that induces immunity which prevents ZIKV vertical transmission and testis damage in mice.

2. Materials and methods

2.1. Cells and antibodies

The African green monkey kidney epithelial cell (Vero; ATCC Cat# CCL-81, RRID: CVCL_0059) and human embryonic kidney cell (293T; ATCC Cat# CRL-3216, RRID: CVCL_0063) were purchased from the American Type Culture Collection (ATCC, Bethesda, MD) and maintained in a high-glucose Dulbecco's modified Eagle's medium (DMEM) supplemented with 10% fetal bovine serum (FBS) (HyClone Laboratories, South Logan, UT) and 1% penicillin/streptomycin (P/S). Cells were cultured at 37 °C with 5% CO₂. Culture medium and antibiotics were purchased from ThermoFisher Scientific (Waltham, MA).

The following antibodies were used in this study: a mouse monoclonal antibody (mAb) 4G2 (ATCC Cat# HB-112, RRID: CVCL_J890) cross-reactive with flavivirus E protein, a mouse polyclone antibody against ZIKV NS5 (in-house generated using the recombinant ZIKV NS5 protein purified from *E.coli.*), ZIKV-specific HMAF (hyper-immune ascitic fluid; obtained from the World Reference Center of Emerging Viruses and Arboviruses [WRCEVA] at the University of Texas Medical Branch), goat anti-mouse IgG conjugated with horseradish peroxidase (HRP; SeraCare KPL Cat# 474-1806, RRID: AB_2307348), and goat anti-mouse IgG conjugated with Alexa Fluor 568 (Thermo Fisher Scientific Cat# A-11004, RRID: AB_2534072).

2.2. Plasmid construction

The plasmid pFLZIKV-PRV (derived from a single-copy vector pCC1TM [Epicentre, Madison, WI]) [28] was used as a starting vector to construct the DNA-launched plasmids in this study. Firstly, the cDNA sequence of ZIKV strain Cambodian FSS13025 (GenBank accession No. KU955593) and the hepatitis delta virus ribozyme (HDVr) was digested from an infectious clone pFLZIKV [29], and cloned into the pFLZIKV-PRV using restriction enzymes *NotI* and *Clal*, resulting in the plasmid pCC1-T7-ZIKV. Next, the simian virus 40 (SV40) or cytomegalovirus (CMV) promoter sequences were amplified by standard PCR from the pcDNA3.1(+) (ThermoFisher Scientific) and fused with the 5'UTR sequence of ZIKV, respectively. The resulting DNA fragments were cloned into the pCC1-T7-ZIKV plasmid using restriction enzymes *HpaI* and *NheI*, resulting in subclones pCC1-SV40-ZIKVa and pCC1-CMV-ZIKVa. Lastly, the SV40 or bovine growth hormone (BGH) polyadenylation (pA) signal sequences were amplified from the pcDNA3.1 vector and cloned into the pCC1-SV40-ZIKVa and pCC1-CMV-ZIKVa through restriction enzymes *Clal* and *SrfI*, respectively, resulting in plasmids pSV40-ZIKV (short as WT or SV40-WT) and pCMV-ZIKV (short as CMV-WT). The flavivirus-conserved polymerase motif GDD mutation (corresponding to residues Gly664, Asp665, and Asp666 in ZIKV NS5 were mutated to Ala) [30] and the 3'UTR 20 nucleotide deletion (Δ 20) [22] was introduced by overlap PCR and cloned into the plasmid pCC1-SV40-ZIKV through restriction enzymes *EcoRI* and *Clal*, resulting in plasmids pFLZIKV- Δ GDD (short as Δ GDD) and pFLZIKV-3'UTR- Δ 20 (short as Δ 20). Plasmids were propagated in the TransforMax EPI300

Chemically Competent *E. coli* (Epicentre, Madison, WI). This pCC1™ vector-derived plasmid could be induced to generate 10–20 copies/cell using L-arabinose in the *E. coli* strain EPI300. All restriction enzymes were purchased from New England BioLabs (Ipswich, MA). All plasmids were validated through restriction enzyme digestion and Sanger DNA sequencing. All primers were synthesized from Integrated DNA Technologies (Skokie, Illinois) and available upon request.

2.3. DNA transfection

5×10^5 Vero cells or 7×10^5 293T cells per well were seeded into a 6-well plate. The next day, cells were transfected with 4 μ g plasmids by X-tremeGENE 9 DNA transfection reagent (Roche) in 3 ml 2% FBS DMEM medium. From day 1 to 5 post-transfection, 200 μ l of culture fluids were collected daily, centrifuged at 415 \times g for 5 min to remove cell debris and stored at -80°C . Viral titers were determined by plaque assay.

2.4. Plaque assay

1.5×10^5 Vero cells per well were seeded into a 24-well plate. The next day, 100 μ l of undiluted virus sample or series of 10-fold diluted virus samples were added to individual well of cell monolayer. After 1 h of incubation at 37°C with 5% CO_2 , the inoculum in each well was replaced with 0.6 ml of overlay medium (DMEM medium supplemented with 2% FBS and 0.8% methylcellulose [Sigma]). After incubation at 37°C with 5% CO_2 for 4 days, cells were fixed in 3.7% formalin solution and stained with 1% crystal violet. For ZIKV Δ 20 mutant viruses, viral titers were determined by focus-forming assay as described previously [22].

2.5. Immunofluorescence assay (IFA)

8×10^4 Vero Cells were seeded into each well of an 8-well Lab-Tek II chamber slide (Thermo Fisher Scientific). The next day, cells were transfected with 0.5 μ g of DNA per well. At selected time points, cells were fixed with chilled methanol at -20°C for 30 min. After 1 h incubation in blocking buffer (PBS supplemented with 1% FBS and 0.05% Tween-20), cells were incubated with the primary antibody 4G2 for 1 h. After three PBS washes, cells were incubated with goat anti-mouse IgG conjugated with Alexa Fluor 568 (1:1000 diluted in blocking buffer) for 1 h. Finally, after three PBS washes, cells were mounted in a Vectashield mounting medium with DAPI (Vector Laboratories). Fluorescence images were acquired under Eclipse Ti2 inverted fluorescence microscope (Nikon Instruments Inc.).

2.6. SDS-PAGE and western blot

Cells from the 6-well plates were washed once with PBS and lysed at 4°C for 1 h in 200 μ l RIPA lysis buffer (ThermoFisher Scientific) supplemented with 1 \times complete protease inhibitor cocktail (Roche). Lysates were centrifuged at 20,000 \times g and 4°C for 30 min to remove cell debris. Supernatants were collected and mixed with 4 \times LDS sample buffer (ThermoFisher Scientific). After denaturing at 70°C for 15 min, 10 μ l samples were loaded onto to a 12% Mini-Protean TGX Stain-Free Precast gel (Bio-Rad Laboratories). After separation by electrophoresis, proteins were transferred onto a polyvinylidene difluoride (PVDF) membrane using a Trans-Blot Turbo Transfer System (Bio-Rad Laboratories). The blot was firstly incubated at room temperature for 1 h in a blocking buffer containing TBST (10 mM Tris-HCl [pH 8.0], 150 mM NaCl, and 0.1% Tween 20) and 5% skim milk, followed by 1 h of incubation with primary antibody (1:1000 dilution in blocking buffer). After three TBST-buffer washes, the blot was incubated with the goat anti-mouse IgG conjugated to HRP (1:10,000 dilution in blocking buffer). After another three TBST-buffer washes, the blot was incubated with SuperSignal™ West Femto Maximum Sensitivity Substrate (Thermo Fisher Scientific).

Chemiluminescence signals were detected in ChemiDoc System (Bio-Rad).

2.7. RT-PCR and sequencing

Viral RNAs in culture fluids (140 μ l) or mouse serum were used for viral RNA extraction by QIAamp viral RNA mini kit (Qiagen). RT-PCR assays were performed using SuperScript III One-Step RT-PCR System with Platinum Taq DNA Polymerase kit (Life technologies) following the manufacturer's protocols. Six cDNA fragments covering the entire genome of ZIKV were amplified by RT-PCR, purified and subjected to Sanger sequencing at GENEWIZ (South Plainfield, NJ).

2.8. ZIKV/mCherry neutralization assay

Titers of neutralizing antibody in mouse serum were determined by using a ZIKV/mCherry infection assay as described previously [22,23]. Briefly, sera were 2-fold serially diluted (starting at 1:25 dilution) in culture medium (containing 2% FBS) and then incubated with equal volume of ZIKV/mCherry reporter viruses at 37°C for 1 h. Afterwards, antibody-virus complexes were added to Vero cell monolayers in a 96-well plate. At 48 h post-infection, mCherry fluorescence-positive cells were quantified by Cytation 5 Cell Imaging Multi-Mode Reader (Biotek). Fluorescence-positive cells from serum-treated wells were normalized to those of non-treatment controls (set as 100%). The effective dilution of sera to reduce the percentage of mCherry-positive cells by 50% (NT_{50}) was calculated using nonlinear regression analysis in GraphPad Prism 7 software (La Jolla, CA).

2.9. Mouse experiment

All animal studies were performed as approved by the University of Texas Medical Branch (UTMB) Institutional Animal Care and Use Committee (IACUC). All efforts were made to minimize animal suffering. Plasmid DNA was diluted to indicated concentration in calcium/magnesium-free phosphate-buffered saline (DPBS, ThermoFisher Scientific) and administrated into A129 mice by intramuscular (IM) injection or by IM injection together with electroporation (IM&EP) using the TriGrid™ Delivery System (Ichor Medical Systems, San Diego, CA) as described previously [31]. The A129 mouse is a model susceptible to ZIKV infection [32]. For consistent dosing by TriGrid™ device, six-week-old mice A129 mice with weight above 15 g were chosen for this study. Briefly, after anesthetized with isoflurane gas, mice were injected into one tibialis anterior muscle with 20 μ l of DNA solution using a 3/10 ml U-100 insulin syringe (Becton-Dickinson, Franklin Lakes, NJ) inserted into the center of a TriGrid electrode array with 2.5 mm electrode spacing. Mock-infected mice were given DPBS by the same route. Injection of DNA was followed immediately by electrical stimulation at an amplitude of 250 V/cm, and the total duration was 40 ms over a 400-ms interval. The control intramuscular injection was performed as described above without the application of electrical stimulation.

After immunization, mice were monitored for weight loss and signs of disease daily. At selected time points, mice were bled *via* the retro-orbital sinus (RO) and viremia was determined by plaque assay. Neutralizing antibodies in sera were measured using ZIKV/mCherry infection assay. Mice were challenged on day 29 post-immunization with parental ZIKV strain PRVABC59 (10^6 PFU) *via* the subcutaneous route. On day 2 post challenge, mice were bled and viremia were determined by plaque assay. Sperm counting was performed according to the protocol as described previously [23]. Mice were euthanized and necropsied at indicated time points. Epididymis and testes were harvested immediately. Motile and non-motile sperms were counted manually on a hemocytometer by microscopy. Total sperm counts equal to the sum of motile and non-motile sperms.

For the mouse pregnancy study, the same IM&EP procedures were applied to administer the DNA solution into six-week old female mice.

On day 29 post-immunization, mice were bled for measuring NT₅₀. Mice were mated starting on day 30 post-immunization. Mouse embryonic development started (E0.5) once mouse vaginal plugs were observed. At E10.5, mice were challenged with parental ZIKV strain PRVABC59 (10⁶ PFU) *via* the subcutaneous route. At E12.5, mice were bled to measure viremia. At E18.5, all dams were euthanized and maternal tissues (brain, spleen and placenta) and fetus were harvested. Fetal weight was measured immediately. After decapitation, fetal heads and blood were collected. Mouse tissues were homogenized in 500 µl of DMEM medium using TissueLyser II (Qiagen) for 5 min at 30 Hz. After centrifugation at 15000 × rpm for 10 min, supernatants were harvested. Plaque assays were performed on Vero cells to determine virus loads in maternal brain, spleen and placenta, and fetal head. Neutralizing antibodies in fetal serum were measured using ZIKV/mCherry neutralization assay as described above.

2.10. Intracellular cytokine staining (ICS)

Approximately 2.5 × 10⁶ splenocytes were stimulated with 1 × 10⁵ IFU of live ZIKV (strain FSS13025) for 24 h or 10 µg/ml E peptide (Sequence 294–302 in ZIKV polyprotein) [33] for 5 h. Live ZIKV was used as a stimulant for measuring both CD4⁺ and CD8⁺ T cell response [22]. The E peptide was used as stimulant for measuring CD8⁺ T cell response [33]. During the final 5 h of stimulation, BD GolgiPlug (BD Bioscience) was added to block protein transport. Cells were stained with antibodies against surface markers CD3 (APC-conjugated) and CD4 (FITC-conjugated) or CD8 (FITC-conjugated). Afterwards, cells were fixed in 2% paraformaldehyde and permeabilized with 0.5% saponin. Cells were then incubated with PE-conjugated anti-IFN-γ and PE-Cy7-conjugated anti-TNF-α antibodies or control PE-conjugated rat IgG1. Samples were processed with a BD Accuri™ C6 Flow Cytometer instrument. Dead cells were excluded on the basis of forward and side light scatter. Data were analyzed with a CFlow Plus Flow Cytometer (BD Biosciences).

2.11. Bio-Plex immunoassay

Approximately 3 × 10⁵ splenocytes per well were plated in a 96-well plate and stimulated with 2 × 10⁴ FFU of ZIKV (strain FSS13025) for 2 days, respectively. Culture supernatants were harvested and frozen at −80 °C. Cytokines IL-2, IFN-γ and TNF-α in the culture supernatants were measured using a Bio-Plex Pro Mouse Cytokine Assay (Bio-Rad, Hercules, CA) according to the manufacturer's instructions.

2.12. Data process and analysis

Images were processed in software ImageJ (NIH). Data were analyzed in GraphPad Prism 7.0 software (La Jolla, CA). Results were presented as the mean ± standard deviation unless indicated separately. Comparisons of groups were performed using multiple *t*-test, unpaired nonparametric Mann-Whitney unpaired test or one-way ANOVA test. **p* < 0.05, significant; ***p* < 0.01, very significant; ****p* < 0.001, highly significant; *****p* < 0.0001, extremely significant; n.s., not significant. Figures were assembled using Adobe illustrator.

3. Results

3.1. Construction and characterization of plasmid DNA-LAV in cell culture

We chose to convert ZIKV-3'UTR-Δ20 (a LAV candidate containing a 20-nucleotide deletion within the 3'UTR of the ZIKV genome) into a plasmid DNA-launched LAV. ZIKV-3'UTR-Δ20 has an excellent safety and efficacy profile: a single-dose vaccination of 10³ FFU confers sterilizing immunity in NHPs [23]. To convert it to a plasmid-launched LAV, we selected the pCC1™ vector to clone the cDNA of ZIKV-3'UTR-Δ20 because its copy number can be conditionally controlled in *E. coli*: (i) A

single copy per cell to maximize the plasmid stability during cloning and (ii) 10–20 copies per cell to increase plasmid yield during production [34]. A eukaryotic promoter was engineered at the 5' end of ZIKV-3'UTR-Δ20 cDNA to launch the transcription of viral RNA through cellular RNA polymerase II (Fig. 1a). A hepatitis delta virus ribozyme (HDVr) sequence and a polyA-signal sequence were engineered at the 3' end of ZIKV-3'UTR-Δ20 cDNA for generation of the authentic 3' end of the viral RNA and for transcription termination (Fig. 1a). The resulting plasmid is named as pZIKV-3'UTR-Δ20. As controls, we also cloned the cDNA of wild-type (WT) ZIKV and a viral polymerase-defective mutant (containing an active site GDD → AAA mutation, defined as ΔGDD) into the pCC1™ plasmid, resulting in pZIKV-WT and pZIKV-ΔGDD, respectively.

We initially determined which eukaryotic promoter should be selected to launch the LAV viral replication in cells. Using pZIKV-WT, we compared the efficiencies of two commonly used eukaryotic promoters (SV40 and CMV) to launch ZIKV (Supplementary Fig. 1a). After transfecting pZIKV-WT DNA into Vero and 293 T cells, the SV40 promoter launched ZIKV more rapidly than the CMV promoter in both cell lines from days 2 to 3 (Supplementary Fig. 1b). This result prompted us to engineer the SV40 promoter to pZIKV-3'UTR-Δ20 (Fig. 1a). Once the SV40-driven pZIKV-3'UTR-Δ20 was constructed, we characterized its ability to launch replication of the LAV virus in cell culture. Upon transfection into Vero cells, pZIKV-3'UTR-Δ20 generated viral E protein-positive cells (Fig. 1b), viral NS5 protein (Fig. 1c), and high titers of LAV virus (peak viral titer of 2 × 10⁶ PFU/ml; Fig. 1d). Compared with pZIKV-WT, pZIKV-3'UTR-Δ20 produced fewer E-positive cells (Fig. 1b) and less NS5 protein (Fig. 1c) in transfected cells. The recovered ZIKV-3'UTR-Δ20 virus exhibited smaller focus morphology than the WT ZIKV (Fig. 1e). As a negative control, cells transfected with the replication-defective pZIKV-ΔGDD did not generate any detectable viral proteins or virus (Fig. 1B-E). These results demonstrate that pZIKV-3'UTR-Δ20 DNA is able to efficiently launch LAV virus in cell culture.

3.2. Immunogenicity and efficacy in A129 mice

We evaluated the immunogenicity and efficacy of the pZIKV-3'UTR-Δ20 DNA in A129 mice [32], which are deficient in interferon-α/β receptors. We chose the TriGrid™ to deliver the plasmid to mice because (i) this device combines intramuscular injection with electroporation and (ii) it has already been successfully used in clinical trials [35]. Fig. 2a outlines the experimental design. A single dose of 0.01, 0.1, or 1 µg of pZIKV-3'UTR-Δ20 DNA was administered to the *tibialis anterior* muscle of six-week-old A129 mice. As controls, mice were administered replication-defective pZIKV-ΔGDD (10 µg), which was expected to yield translation of transcribed ZIKV RNA but not subsequent viral replication, or DPBS. After immunization, all mice remained healthy with no detectable pathologic changes at the site of injection or adverse effects including no weight loss (Fig. 2b). Viremia of <10⁴ PFU/ml was detected in each of the three pZIKV-3'UTR-Δ20-dosed groups (Fig. 2c–f), although the 1-µg dosed group exhibited a higher viremia-positive rate (88%) than the 0.1-µg (25%) and 0.01-µg (27%) groups (Fig. 1k). Sequencing of the viral RNA from mouse sera collected during viremia showed the engineered 20-nucleotide deletion at the 3'UTR without other mutations. Seroconversion rates of 100%, 75%, and 27% were observed from the 1-µg, 0.1-µg, and 0.01-µg pZIKV-3'UTR-Δ20 groups, respectively (Fig. 1k). For each seroconverted mouse, pZIKV-3'UTR-Δ20 DNA rapidly elicited high neutralizing antibody titers of almost 10⁴ within 14–21 days post-immunization (Fig. 2g–i). Upon challenge with 10⁶ PFU of a WT ZIKV strain PRVABC59 from the Puerto Rico epidemic, on day 29 post-immunization, all seroconverted mice were fully protected against infection (Fig. 2c–e), whereas the seronegative mice generated viremia on day 2 post-challenge. Notably, the challenge did not boost the neutralizing antibody titers of seroconverted mice, as indicated by no statistical difference between the neutralizing antibody titers on days 29 and 43 (Fig. 2g–i). As a negative control, immunization with 10 µg of pZIKV-

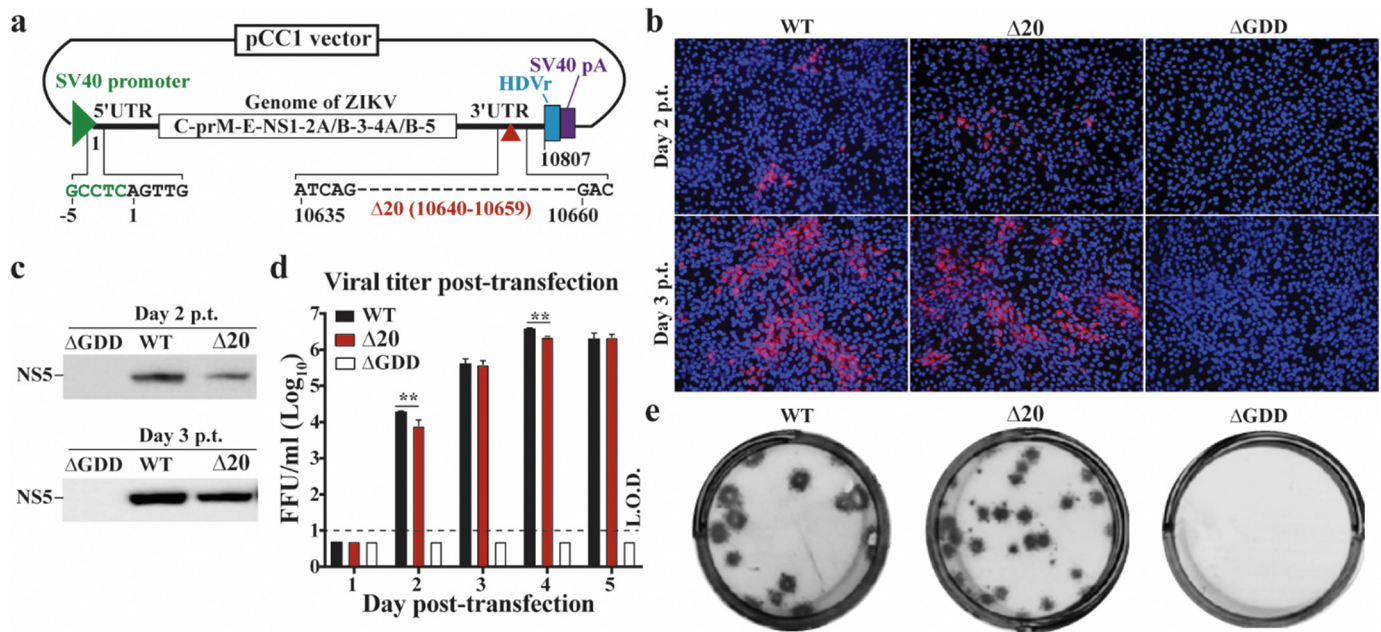


Fig. 1. Characterization of pZIKV-3'UTR-Δ20 in cell culture. (a) Diagram of plasmid pZIKV-3'UTR-Δ20. The plasmid pCCI™ vector was used to engineer a gene cassette containing a promoter from simian virus 40 (SV40), ZIKV-3'UTR-Δ20 cDNA, hepatitis delta virus ribozyme (HDVr) sequence, and SV40 polyadenylation (pA) signal element. Junction sequences are depicted between the SV40 promoter and the 5'UTR of viral genome. The 20-nucleotide deletion at the 3'UTR of ZIKV genome is indicated by a dotted line and nucleotide positions (GenBank accession No. KU955593). (b) Immunofluorescent assay (IFA). Vero cells were transfected with pZIKV-WT, pZIKV-3'UTR-Δ20 (Δ20), or pZIKV-ΔGDD (ΔGDD). At the indicated time post-transfection (p.t.), the cells were stained with 4G2 antibody to detect viral E protein expression (green). Nuclei were counterstained with DAPI (blue). (c) Western blot. The transfected Vero cells were examined for viral NS5 protein expression using Western blot. (d) Virus production post-transfection. Supernatants from the transfected Vero cells were quantified for infectious ZIKV using a focus-forming assay. The dotted line indicates the limit of detection (L.O.D.) of 10 FFU/ml. Multiple *t*-test was performed to analyze the statistical significances. (e) Focus-forming morphologies of WT ZIKV and ZIKV-3'UTR-Δ20 virus. No infectious virus was detected from the pZIKV-ΔGDD-transfected cells.

ΔGDD DNA conferred no viremia post-immunization (Fig. 2f), no neutralizing antibodies before challenge (Fig. 2j), and no protection against challenge (Fig. 2f). Taken together, the results indicate that a single dose of pZIKV-3'UTR-Δ20 is able to rapidly elicit sterilizing immunity (defined as no detectable infectious viruses and no increase of neutralizing antibody titers after challenge) that confers complete protection against ZIKV infection.

3.3. Minimal dose for 100% seroconversion and protective immunity

To determine the minimal dose required for 100% seroconversion, we immunized A129 mice with 0.3 or 0.5 μg of pZIKV-3'UTR-Δ20 (Supplementary Fig. 2a). All 10 mice from the 0.5-μg group and 14 out of 15 mice from the 0.3-μg group developed viremia during days 6–10 post-immunization (Supplementary Fig. 2b, c, f), and elicited high titers of neutralizing antibodies (about 10⁴) from day 14 to 29 post-immunization (Supplementary Fig. 2d–f). Consistently, all seroconverted mice were fully protected against infection (Supplementary Fig. 2b & c), whereas the seronegative mouse from the low-dose (0.3 μg) group generated viremia on day 2 post-challenge (data not shown). The challenge did not boost neutralizing antibody titers in any seroconverted mice (compare the neutralizing antibody titers on days 29 and 43 in Supplementary Fig. 2d & e). The results demonstrate that immunization of 0.5 μg pZIKV-3'UTR-Δ20 DNA is sufficient to confer 100% seroconversion and protective immunity.

3.4. Attenuation of pZIKV-3'UTR-Δ20 in the A129 mice

To validate whether the DNA-launched LAV is attenuated *in vivo*, we compared the viremia and neutralizing antibody development between the pZIKV-3'UTR-Δ20 and pZIKV-WT in A129 mice (Supplementary Fig. 3a). After immunizing mice with 1 μg of plasmid DNA, neither pZIKV-3'UTR-Δ20 (Fig. 2b) nor pZIKV-WT caused weight loss, disease, or death (Supplementary Fig. 3b). This is not surprising because ZIKV-

inflicted morbidity and mortality are age-dependent in A129 mice [32]. We were not able to use younger mice because their *tibialis anterior* muscles are too small for consistent dosing by the TriGrid™. Each pZIKV-WT-immunized mouse developed robust viremia (Supplementary Fig. 3c) and high neutralizing antibody titers (Supplementary Fig. 3d). The average viremia titers in the pZIKV-WT-immunized group were significantly higher than those in the pZIKV-3'UTR-Δ20-immunized group (Supplementary Fig. 3e). The results indicate that the pZIKV-3'UTR-Δ20 launched lower viremia than pZIKV-WT *in vivo*.

3.5. Requirement of TriGrid™ for efficient DNA delivery

To demonstrate the importance of TriGrid™ for efficient DNA delivery, we examined the immunization efficiency using the traditional intramuscular needle injection without electroporation. A129 mice were intramuscularly needle injected with 1 μg of pZIKV-WT and pZIKV-3'UTR-Δ20, then analyzed for viremia and neutralizing antibodies (Supplementary Fig. 4a). After needle injection, 40% (*n* = 6/15) of the pZIKV-WT-immunized animals showed viremia (Supplementary Fig. 4b & f) and 47% (*n* = 7/15) seroconverted (Supplementary Fig. 4d & f), whereas 20% (*n* = 3/15) of the pZIKV-3'UTR-Δ20-immunized mice showed viremia (Supplementary Fig. 4c & f) and 33% (*n* = 5/15) seroconverted (Supplementary Fig. 4e&f). Correlation analysis showed that all mice with detectable viremia after immunization were seroconverted (data not shown). These results demonstrate that, compared with TriGrid™, needle injection alone is much less efficient in DNA delivery, as reflected by viral replication and immunogenicity. Thus, all subsequent mouse experiments were performed using the TriGrid™ device.

3.6. Protection from ZIKV-induced damages to testes

Since ZIKV infection can persist in the male reproductive tract and lead to sexual transmission [36–38], we examined the ability of

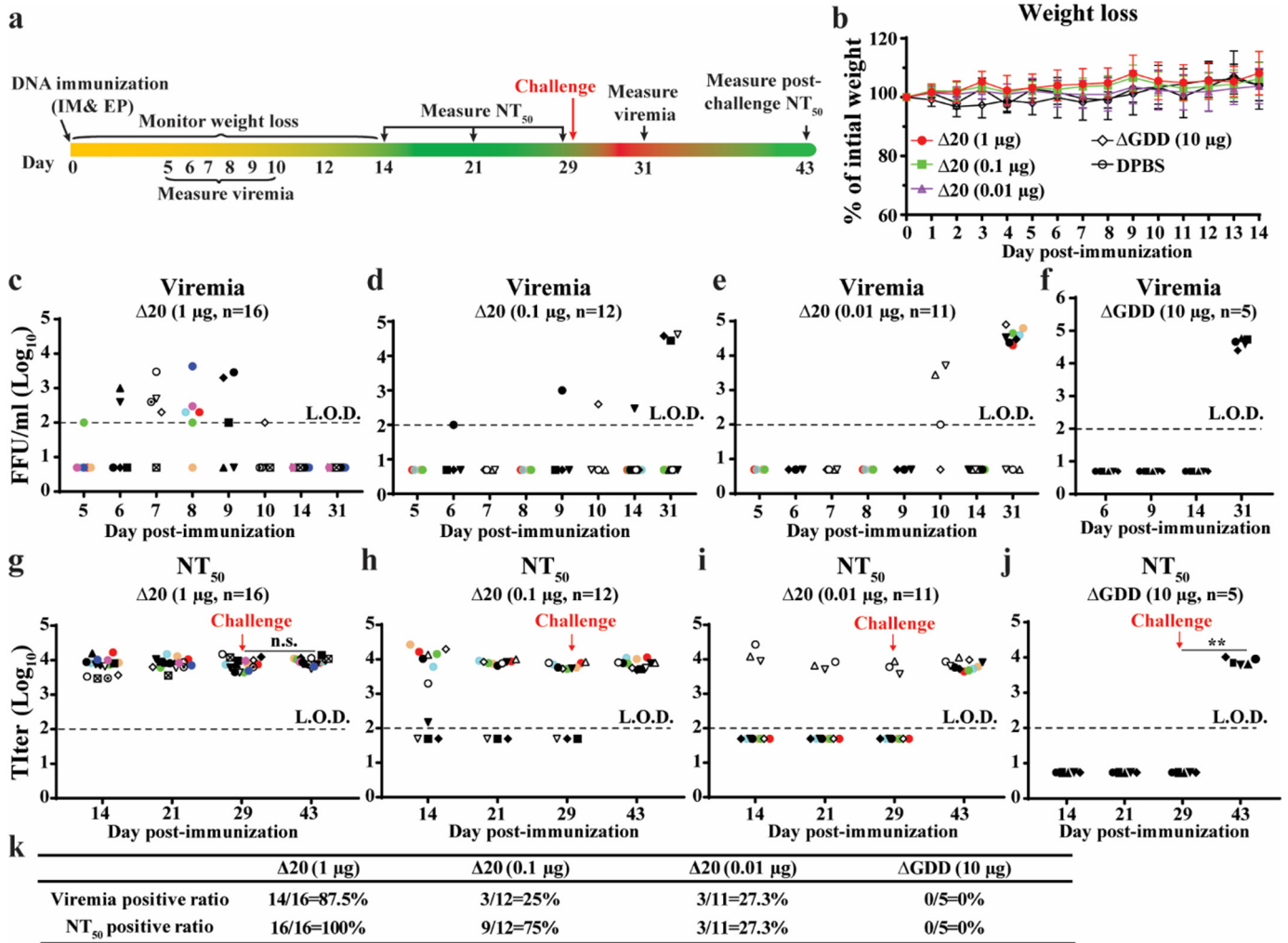


Fig. 2. Immunization of pZIKV-3'UTR- $\Delta 20$ protects the A129 mouse from ZIKV challenge. (a) Experimental design. Various doses of pZIKV-3'UTR- $\Delta 20$ (1, 0.1, 0.01 μg), pZIKV- ΔGDD (10 μg), or DPBS (sham) were inoculated to six-week-old A129 mice via intramuscular (IM) injection and electroporation (EP) using TriGrid™. Following immunization, mice were monitored for weight loss over 14 days. Since our IACUC protocol only allows four blood draws per mouse over 28 days post-transfection (or infection), blood draws were staggered for different mouse sub-cohorts to cover the sampling period of days 5–10 post-immunization. Mice were bled at indicated time for measuring neutralizing antibody titers (NT₅₀) using an mCherry-ZIKV neutralization assay. On day 29 post-immunization, the mice were challenged with 10⁶ PFU of ZIKV strain PRVABC59 via the subcutaneous route (indicated by a red arrow). At indicated time, the mice were bled for measuring viremia using a focus-forming assay. (b) Mouse weight post-immunization. (c–f) Viremia for the mouse groups immunized with 1 μg pZIKV-3'UTR- $\Delta 20$ (c), 0.1 μg pZIKV-3'UTR- $\Delta 20$ (d), 0.01 μg pZIKV-3'UTR- $\Delta 20$ (e), or 10 μg pZIKV- ΔGDD (f). (g–j) Neutralizing antibody titers (NT₅₀) from the mouse groups immunized with 1 μg pZIKV-3'UTR- $\Delta 20$ (g), 0.1 μg pZIKV-3'UTR- $\Delta 20$ (h), 0.01 μg pZIKV-3'UTR- $\Delta 20$ (i), or 10 μg pZIKV- ΔGDD (j). Group sizes (n number) are indicated. Individual mice are indicated by different colors and symbols. Paired t-test was performed to indicate no significant difference (n.s.) between the pre-challenge (day 29) and post-challenge (day 43) neutralizing antibody titers in (g). (k) Summary of viremia-positive and neutralizing antibody-positive ratios for all mouse groups. Limits of detections (L.O.D., dotted lines) of focus-forming assay and neutralization assay (NT₅₀) were 100 FFU/ml and 100-fold dilution, respectively.

pZIKV-3'UTR- $\Delta 20$ to prevent testis infection and injury in A129 mice. First, we tested the safety of pZIKV-3'UTR- $\Delta 20$ in males (Fig. 3). Six-week-old male mice were immunized with 1 μg of pZIKV-3'UTR- $\Delta 20$, 1 μg of pZIKV-WT, or DPBS. On day 29 post-immunization, pZIKV-3'UTR- $\Delta 20$ and pZIKV-WT elicited comparable levels of neutralizing antibody titers (Fig. 3b). No infectious virus was detected in brains (Fig. 3c), spleens (Fig. 3d), or testes (Fig. 3e) of pZIKV-3'UTR- $\Delta 20$ -, pZIKV-WT- or DPBS-immunized mice. Notably, one testis from each of the pZIKV-WT-immunized animals suffered significant weight loss compared with the other testis (Fig. 3f & g). In addition, the pZIKV-WT-immunized animals showed significantly lower total sperm counts (Fig. 3h) and motile sperm counts (Fig. 3i). In contrast, mice immunized with pZIKV-3'UTR- $\Delta 20$ or DPBS did not exhibit any weight loss or oligospermia (Fig. 3f–i). We currently don't know what contributed to the uneven weight loss of testis pair from the pZIKV-WT-immunized animals. Nevertheless, the results suggest that pZIKV-3'UTR- $\Delta 20$ immunization does not cause persistent infection or oligospermia.

Next, we tested the efficacy of pZIKV-3'UTR- $\Delta 20$ in preventing testis infection and damage (Fig. 4A). Six-week-old A129 male mice were immunized with 1 μg of pZIKV-3'UTR- $\Delta 20$ or DPBS. By day 29 post-immunization, pZIKV-3'UTR- $\Delta 20$ elicited robust neutralizing antibody titers of 10⁴ (Fig. 4b). On the same day, mice were challenged with 10⁶ PFU of ZIKV PRVABC59 by the subcutaneous route. On day 2 post-challenge, no viremia was detected in the pZIKV-3'UTR- $\Delta 20$ -immunized mice, whereas mean viremia of 3 × 10⁴ PFU/ml was detected in the DPBS-immunized group (Fig. 4c). In agreement with the results presented in Fig. 2g, the challenge did not significantly boost neutralizing antibody titers measured on day 14 post-challenge (Fig. 4b). On day 21 post-challenge, we analyzed organ viral loads and testis damage. For the pZIKV-3'UTR- $\Delta 20$ -immunized group, no virus was detected in brains (Fig. 4d), spleens (Fig. 4e), or testes (Fig. 4f); no weight loss of testes (Fig. 4g & h) or decrease in total and motile sperm counts (Fig. 4i & j) were observed. In contrast, after challenge, 40% (n = 2/5) of the control PBS-immunized mice had virus in the testes (Fig. 4f), smaller testes

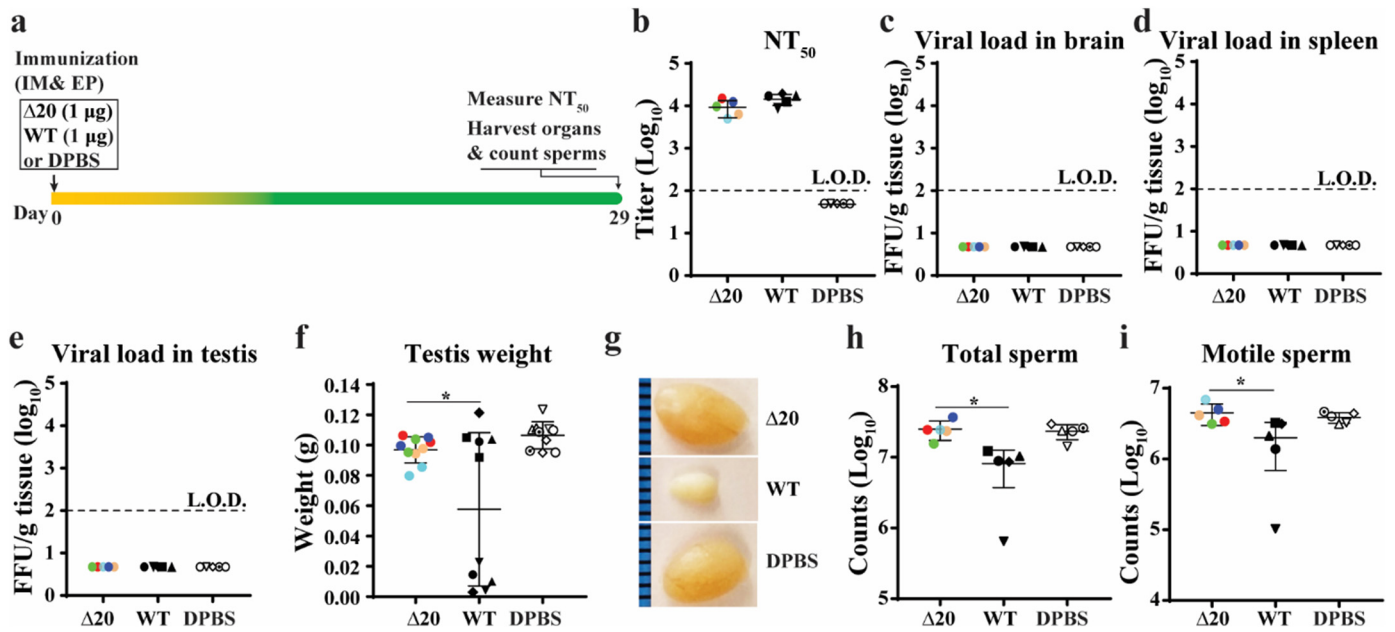


Fig. 3. Safety of pZIKV-3'UTR- Δ 20 in male mice. (a) Experimental design. Six-week-old male A129 mice were immunized with pZIKV-3'UTR- Δ 20 (1 μ g), pZIKV-WT (1 μ g), or DPBS (sham) via intramuscular (IM) injection and electroporation (EP) using TriGrid™. On day 29 post-immunization, mice were sacrificed for analysis. Neutralizing antibody titers were measured on day 29 post-immunization using an mCherry ZIKV neutralization assay (b). Viral loads in mouse brain (c), spleen (d), and testis (e) were determined by a focus-forming assay. The L.O.D.s for organ viral load and NT₅₀ were 100 FFU/g tissue and 100-fold dilution, respectively. (f) Testis weight. (g) Representative images of testes from each group. The epididymis was harvested for counting total sperm (h) and motile sperm (i). Individual mice are indicated by different colors and symbols. The means and standard deviations are shown. A one-way analysis of variance (ANOVA) test was performed to determine the statistically significant differences among groups.

(Fig. 4g & h), and oligospermia (Fig. 4i & j). Collectively, the data indicate that pZIKV-3'UTR- Δ 20 immunization prevents testis infection and oligospermia.

3.7. Prevention of vertical transmission in pregnant mice

To test the ability of pZIKV-3'UTR- Δ 20 to prevent *in utero* transmission, we immunized six-week-old A129 female mice with 1 μ g of pZIKV-3'UTR- Δ 20 or DPBS (Fig. 5a). The immunized mice developed high neutralizing antibody titers of 5.6×10^3 on day 29 post-immunization (Fig. 5b). Female mice were then mated with males on days 30–37 post-immunization, and examined for pregnancy [indicated by vaginal plugs observed after mating and defining embryonic day 0.5 (E0.5)]. At E10.5, the pregnant mice were challenged with 10^6 PFU of ZIKV PRVABC59 by the subcutaneous route. No viremia was detected in the pZIKV-3'UTR- Δ 20-immunized mice on day 2 post-challenge, whereas viremia of 1.7×10^5 PFU/ml was observed in the control DPBS-immunized group (Fig. 5c). At E18.5, the pregnant mice were measured for viral loads in maternal and fetal organs. For the pZIKV-3'UTR- Δ 20-immunized group, no infectious virus was detected in maternal brains (Fig. 5d), spleens (Fig. 5e), placentas (Fig. 5f), or in fetal heads (Fig. 5g). Normal fetal weights were observed in the pZIKV-3'UTR- Δ 20-immunized mice (Fig. 5h). In contrast, in the DPBS-immunized and challenged group, infectious virus was found in 100% ($n = 5/5$) of maternal brains (Fig. 5d), 40% ($n = 2/5$) of maternal spleens (Fig. 5e), 100% ($n = 35/35$) of placentas (Fig. 5f), and 6% ($n = 2/35$) of fetal heads (Fig. 5g). In addition, significant fetal weight loss was observed in the DPBS-immunized and challenged group.

Next, we asked whether maternal antibodies could be transferred to fetuses after immunization. Indeed, high neutralizing antibody titers of 3.8×10^3 were detected from the fetal serum (Fig. 5i). Taken together, the results demonstrate that a single-dose immunization of pZIKV-3'UTR- Δ 20 protects maternal organs from infection and prevents maternal-to-fetal transmission.

3.8. T cell response after pZIKV-3'UTR- Δ 20 immunization

T cell immunity plays an important role in preventing ZIKV infection [33]. We examined T cell responses in A129 mice immunized with 0.5 μ g of pZIKV-3'UTR- Δ 20 or DPBS. Mouse spleens were harvested on day 29 post-immunization. Splenocytes were cultured *ex vivo*, stimulated with a previously reported ZIKV E peptide [33] or infectious WT ZIKV, and analyzed by an intracellular cytokine staining (ICS) assay and a Bio-Plex immunoassay. The pZIKV-3'UTR- Δ 20-immunized animals had significantly more ZIKV-specific IFN- γ ⁺ and IFN- γ ⁺ TNF- α ⁺ CD4⁺ (Fig. 6a and Supplementary Fig. 5a) and CD8⁺ T cells (Fig. 6b and Supplementary Fig. 5b&c) than the DPBS-vaccinated animals. In addition, splenocytes from the pZIKV-3'UTR- Δ 20-immunized mice produced significantly higher levels of IL-2 (Fig. 6c), IFN- γ (Fig. 6d), and TNF- α (Fig. 6e) proteins than the DPBS-immunized animals upon *ex vivo* re-stimulation with ZIKV. These data indicate that immunization with pZIKV-3'UTR- Δ 20 elicits robust CD4⁺ and CD8⁺ T cell responses in mice.

4. Discussion

Vaccines, especially LAV, have been highly effective in controlling and even eradicating infectious diseases [39]. Enhancing vaccine performance with improved simplicity, immunity, and delivery speed is critical, particularly when responding to epidemic emergency. The goal of this study is to develop and characterize pZIKV-3'UTR- Δ 20 that combines the strengths of DNA vaccines (chemical stability, no cold chain, easy production, and low cost) and LAVs (single dose, quick immunity and durable protection). Our results showed that a single-dose vaccination of ≥ 0.5 μ g of pZIKV-3'UTR- Δ 20 elicited 100% protective immunity within 14–21 days in the A129 mice. The vaccination completely prevented ZIKV infection, vertical transmission during pregnancy, and male reproductive tract infections. However, due to the detection limits of plaque and focus-forming assays used in this study, we could not exclude the possibility of low levels of viral replication after challenge.

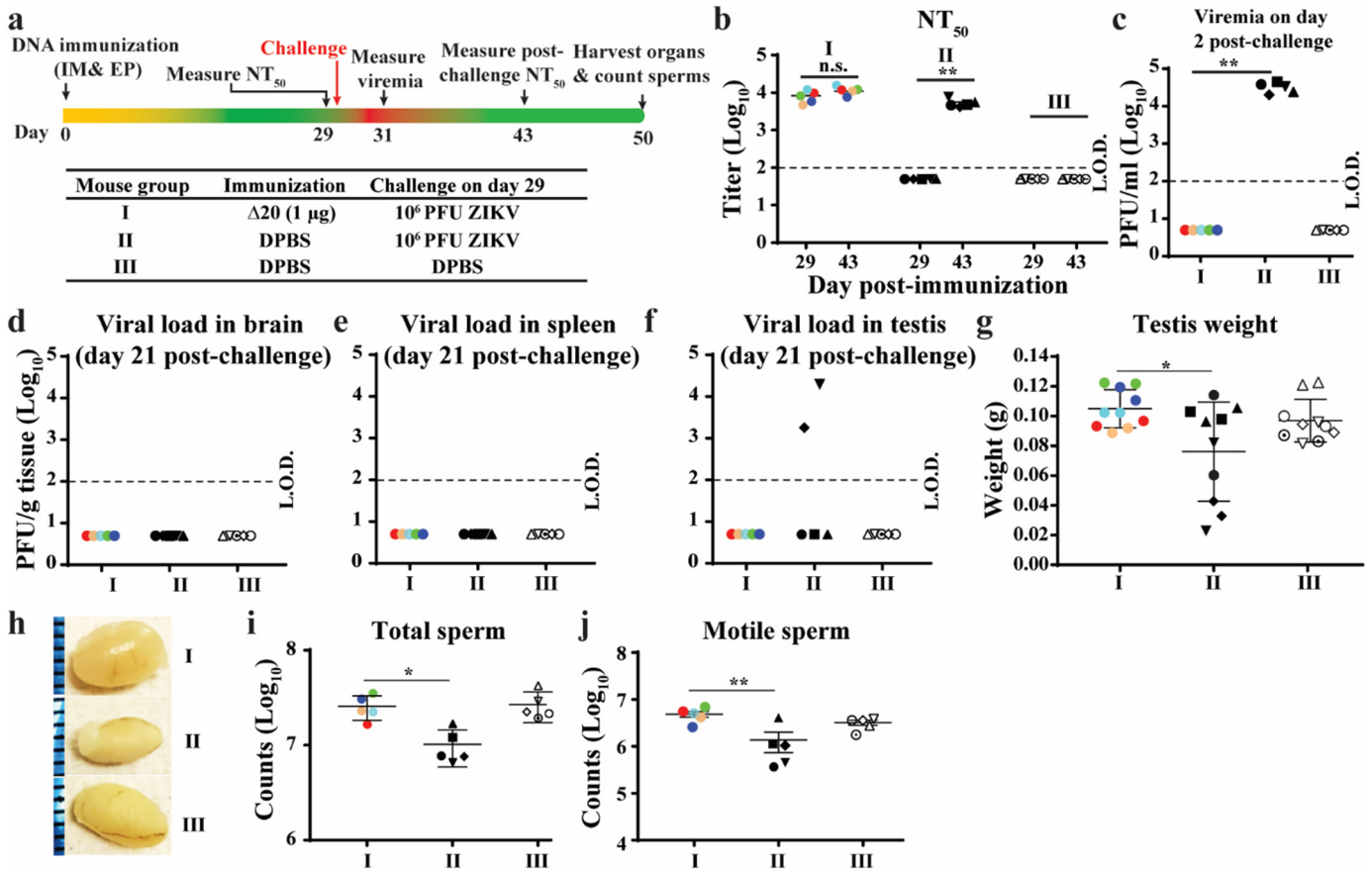


Fig. 4. Immunization with pZIKV-3'UTR-Δ20 protects male mice from ZIKV-induced damages to testis. (a) Experimental design. The bottom panel shows three mouse groups (I, II, and III) with different immunizing agents and challenge conditions. Six-week-old male A129 mice were vaccinated with pZIKV-3'UTR-Δ20 (1 μg) or DPBS (sham) using TriGrid™. On day 29 post-immunization, the mice were challenged with 10⁶ PFU of epidemic ZIKV strain PRVABC59 or DPBS controls. (b) Neutralizing antibody titers on day 29 before challenge and on day 14 post-challenge (equivalent to day 43 post-immunization). Paired t-test was performed to indicate no significant difference (n.s.) between the pre-challenge (day 29) and post-challenge (day 43) neutralizing antibody titers. (c) Viremia on day 2 post-challenge (equivalent to day 31 post-immunization). On day 21 post-challenge, the mice were sacrificed to determine viral loads in brain (d), spleen (e), and testis (f) using a focus-forming assay. (g) Testis weight on day 21 post-challenge. (h) Representative images of testes from each group collected on day 21 post-challenge. The epididymis was harvested for total sperm counts (i) and motile sperm counts (j). Individual mice are indicated by different colors and symbols. A one-way ANOVA test was performed to determine statistically significant differences among groups.

Since RT-PCR test is much more sensitive than the plaque and focus-forming assays (Supplementary Fig. 6), future non-human primate studies should employ RT-PCR assay to detect viral RNA. The RT-PCR assay should also be used in preclinical safety studies to measure viral RNA levels in different organs collected at multiple time points post-vaccination. Besides antibody response, the immunized mice also developed robust T cell responses. The DNA-launched approach could serve as a universal platform to deliver LAVs for other positive-sense, single-stranded RNA viruses. Indeed, such DNA-launched LAVs have been reported for Kunjin virus [40], YFV 17D [41], JEV SA14-14-2 [42], chikungunya virus 181/clone25 strain [43], and Venezuelan equine encephalitis virus TC-83 strain [44]. Compared with previous reports, our study showed lower minimal plasmid dose required for 100% protection (0.5 μg) in mice. More importantly, we report, for the first time, that a DNA-launched LAV is able to elicit sterilizing antibody titers as well as robust T cell responses. These results have clearly demonstrated the strengths of the DNA-launched LAV approach.

DNA and mRNA subunit vaccines (expressing viral prM-E proteins) have been well developed for ZIKV [14–18], among which DNA subunit vaccines have already shown promising safety and immunogenicity in phase I clinical trials [20,21]. Fifty micrograms of subunit DNA [17,18] and 10–30 μg of subunit RNA [14–16] were used in mouse efficacy experiments. These doses are much higher than the 0.5-μg minimal dose required for 100% seroconversion we demonstrated here for pZIKV-3'UTR-Δ20. However, caution should be taken when comparing the doses used in various studies because of different experimental

conditions (e.g., RNA/DNA delivery methods, different promoters used in plasmids, and mouse strains). For practical purposes, lowering the minimal protective dose is desirable for a vaccine, particularly when responding to epidemic emergencies that often require the rapid production of millions of doses for vaccinating large populations. In addition, lower doses of DNA plasmid could minimize potential adverse effects in vaccinees. Thus, future studies should be performed to further improve the delivery efficiency of pZIKV-3'UTR-Δ20 by comparing different DNA delivery devices (e.g., injection/electroporation device from Inovio and needle-free injection device from ParmaJet) and through different routes of administration (e.g., intradermal versus intramuscular). Since several of these DNA delivery devices have already been used in clinical trials, these devices will greatly facilitate the advancement of DNA-launched LAVs to clinics. Due to the large size of DNA-launched LAV plasmid (about 18 kb in the case of pZIKV-3'UTR-Δ20), we think that electroporation may contribute significantly to the efficient delivery of large DNA plasmid into cells. Besides the delivery devices discussed above, nanoparticle technology could also be explored for the efficient delivery of the DNA-launched LAVs. Such nanoparticle formulations have to be co-developed with the DNA-launched LAVs in pre-clinics and clinics.

A number of important questions remain to be answered to further develop pZIKV-3'UTR-Δ20 as a vaccine candidate. First, what are the initial cell types that launch ZIKV-3'UTR-Δ20 LAV replication after plasmid electroporation? It is well documented that intramuscular injection with plasmid DNA results in transgene expression primarily in muscle

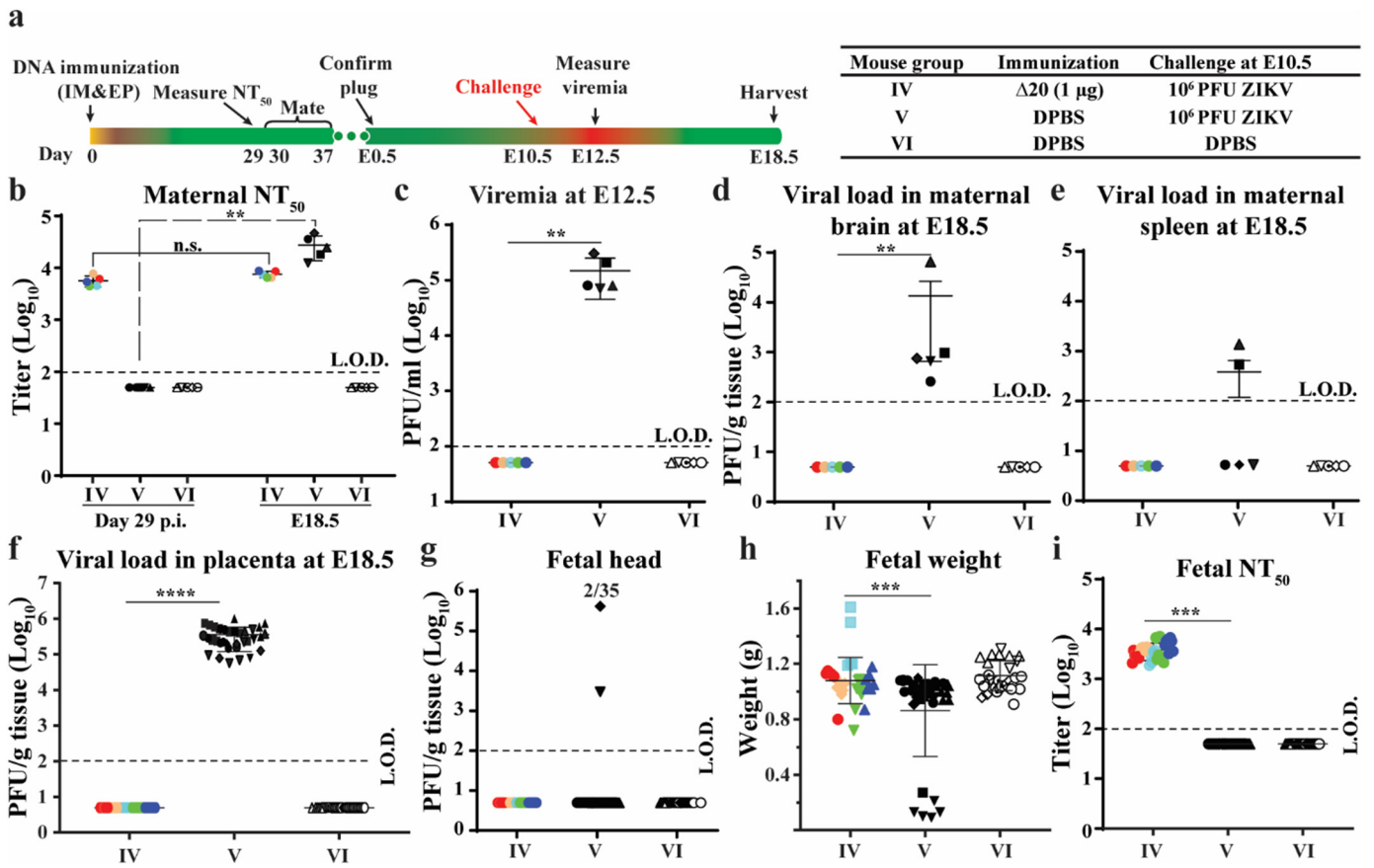


Fig. 5. Prevention of vertical transmission from pregnant mice. (a) Experimental design. The right panel shows three mouse groups (IV, V, and VI) with different immunizing agents and challenge conditions. Six-week-old female A129 mice were immunized with pZIKV-3'UTR- $\Delta 20$ (1 μg) or DPBS (sham) using TriGrid™. At E10.5, mice were challenged with 10^6 PFU of ZIKV strain PRVABC59 or DPBS controls via the subcutaneous route. At E18.5, the mice were sacrificed for measuring viral loads in maternal and fetal organs. (b) Maternal NT₅₀ values on day 29 post-immunization and at E18.5. For mouse group IV, paired t-test was performed to indicate no significant difference (n.s.) between the pre-challenge (day 29) and post-challenge (E18.5) neutralizing antibody titers. (c) Viremia on day 2 post-challenge. (d) Maternal brain viral loads. (e) Maternal spleen viral loads. (f) Placenta viral loads. (g) Fetal head viral loads. (h) Fetal weights. (i) Neutralizing antibodies in fetal blood. Individual dams are indicated by different colors and symbols. Fetuses and their parental mice are matched with the same colors and symbols. The L.O.D.s for viremia, organ virus load, and neutralizing antibody titer are 100 PFU/ml, 100 PFU/g, and 100-fold dilutions, respectively. A one-way ANOVA test was performed to determine statistically significant differences among groups.

cells. Bone marrow-derived dendritic cells are central to the induction of immune response by DNA vaccines [45]. Engineering pZIKV-3'UTR- $\Delta 20$ with a reporter gene (e.g., GFP or mCherry in-frame fused with the viral open-reading-frame) may facilitate tracking the initial

production and spread of the DNA-launched LAV. The same experiment may also be used to estimate the duration of LAV production at the injection site after plasmid vaccination. Second, how long will the protective immunity last after vaccination with pZIKV-3'UTR- $\Delta 20$? In

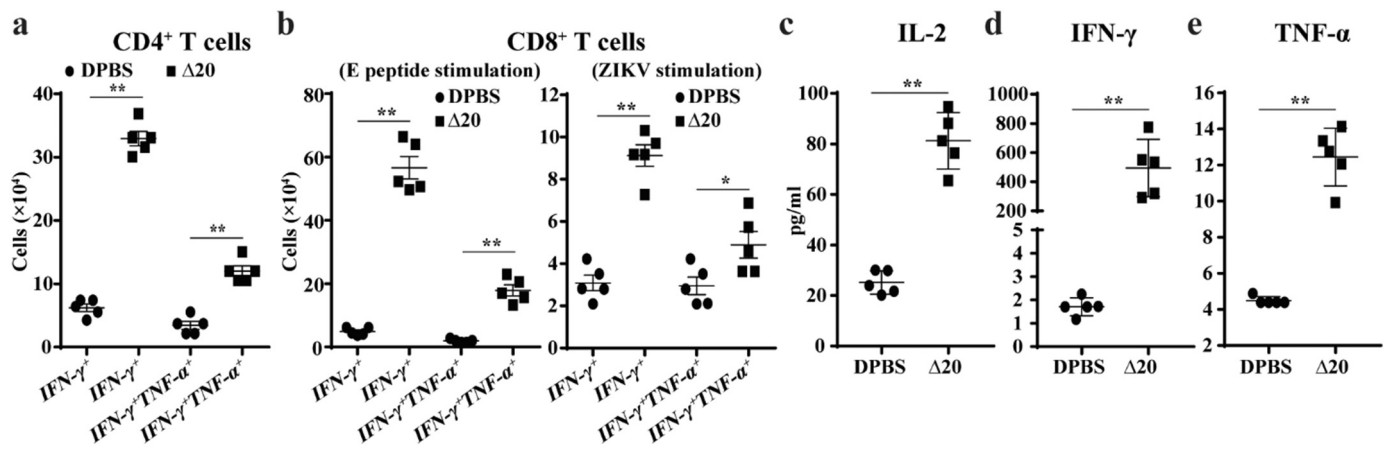


Fig. 6. T cell responses in A129 mice after pZIKV-3'UTR- $\Delta 20$ immunization. Six-week-old A129 mice were immunized with pZIKV-3'UTR- $\Delta 20$ (0.5 μg) or DPBS (sham) using TriGrid™. On day 29 post-immunization, splenocytes were harvested for T cell analysis. (a) Total numbers of CD4⁺ T cell subsets per spleen. Splenocytes were cultured *ex vivo* with ZIKV for 24 h and stained for IFN- γ , TNF- α , and CD4 T cell markers. (b) Total numbers of CD8⁺ T cell subsets. Splenocytes were cultured *ex vivo* with ZIKV for 24 h (right panel) or with an E peptide for 5 h (left panel) and stained for IFN- γ , TNF- α , and CD8 T cell markers. Cytokines IL-2 (c), IFN- γ (d), and TNF- α (e) in cell culture media were measured after splenocytes were stimulated by ZIKV for 2 days. An unpaired nonparametric Mann-Whitney test was performed to analyze statistical significance.

non-human primates, two immunizations with a subunit DNA vaccine resulted in short-lived immunogenicity and efficacy (reduced protection and declining neutralizing antibody titers to sub-protective levels at the end of year one) [46]. Since pZIKV-3'UTR-Δ20 launches LAV virus, the durability of protective immunity after vaccination is expected to be significantly improved. As of today, the neutralizing antibody titers from the 1-μg pZIKV-3'UTR-Δ20-immunized mice remained $>2 \times 10^3$ four months post-immunization (data not shown). Third, maternal neutralizing antibody transfer was observed from the vaccinated dams to fetuses. The transferred maternal antibodies were presumably IgGs because IgMs cannot cross the placenta. It remains to be determined how long the maternally transferred neutralizing activity would last in protecting the newborn mice against infection. Finally, DNA vaccines have repeatedly shown good efficacy in mice, but not in larger animals. Although expression of replicating RNA genome from the DNA-launched platform may improve this outcome, the single-dose mouse efficacy observed here remains to be validated in non-human primates and humans.

In summary, we have developed a plasmid-launched ZIKV LAV that combines the advantages of DNA vaccines and LAVs. A single-dose immunization of our pZIKV-3'UTR-Δ20 induces robust immunity to prevent pregnancy transmission and testis damage in mouse models. Our results suggest that further development of the pZIKV-3'UTR-Δ20 is warranted, and that the plasmid-launched LAV platform could be applied to other plus-sense, single-stranded RNA viruses.

Acknowledgements

We thank Daniele Medeiros for help with a pilot experiment. We also thank colleagues at UTMB for helpful discussions during the course of the project.

Funding sources

J.Z. and X.X. were awarded with postdoctoral fellowships from the McLaughlin Endowment at University of Texas Medical Branch and the Novartis Institutes for BioMedical Research, respectively. P.-Y.S. lab was supported by a University of Texas STARs Award, a Kleberg Foundation Award, UTMB CTSA UL1TR-001439, and NIH grant AI127744. T.W. lab was supported by NIH grant AI099123 and UTMB Sealy Institute for Vaccine Sciences Pilot Grant. This research was also partially supported by NIH grant AI120942 to S.C.W. and by Cooperative Agreement Number U01CK000512 to S.C.W., funded by the Centers for Disease Control and Prevention. Its contents are solely the responsibility of the authors and do not necessarily represent the official views of the Centers for Disease Control and Prevention or the Department of Health and Human Services.

Declaration of interest

J.Z., X.X., and P.-Y.S. filed a provisional patent on the DNA-launched LAV platform. Other authors have no conflict of interest to declare.

Author contributions

J.Z., X.X., L.H., S.C., and A.E.M. performed experiments. J.Z., X.X., L.H., and C.S. analyzed the data. J.Z., X.X., S.C.W., T.W., and P.-Y.S. interpreted the results. J.Z., X.X., S.C.W., W.T., and P.-Y.S. wrote the manuscript.

Appendix A. Supplementary data

Supplementary data to this article can be found online at <https://doi.org/10.1016/j.ebiom.2018.08.056>.

References

- [1] Pierson TC, Diamond MS. Flaviviruses. In: Knipe DM, Howley PM, editors. *Fields virology*, vol. 1., 6th.; 2013. p. 747–94.
- [2] Dick GW, Kitchen SF, Haddock AJ. Zika virus. I. Isolations and serological specificity. *Trans R Soc Trop Med Hyg* 1952;46(5):509–20.
- [3] Aliota MT, et al. Zika in the Americas, year 2: What have we learned? What gaps remain? A report from the Global Virus Network. *Antiviral Res* 2017;144:223–46.
- [4] Ikejezie J, et al. Zika virus transmission - region of the Americas, May 15, 2015–December 15, 2016. *MMWR Morb Mortal Wkly Rep* 2017;66(12):329–34.
- [5] Weaver SC, et al. Zika virus: History, emergence, biology, and prospects for control. *Antiviral Res* 2016;130:69–80.
- [6] Costello A, et al. Defining the syndrome associated with congenital Zika virus infection. *Bull World Health Organ* 2016;94(6) p. 406–406A.
- [7] Hoen B, et al. Pregnancy Outcomes after ZIKV Infection in French Territories in the Americas. *N Engl J Med* 2018;378(11):985–94.
- [8] Dos Santos T, et al. Zika virus and the Guillain-Barre syndrome - case series from seven countries. *N Engl J Med* 2016;375(16):1598–601.
- [9] Shan C, Xie X, Shi PY. Zika virus vaccine: progress and challenges. *Cell Host Microbe* 2018;24(1):12–7.
- [10] Xie X, et al. Small molecules and antibodies for Zika therapy. *J Infect Dis* 2017; 216(suppl_10):S945–50.
- [11] Abbink P, Stephenson KE, Barouch DH. Zika virus vaccines. *Nat Rev Microbiol* 2018.
- [12] Modjarrad K, et al. Preliminary aggregate safety and immunogenicity results from three trials of a purified inactivated Zika virus vaccine candidate: phase 1, randomised, double-blind, placebo-controlled clinical trials. *Lancet* 2018; 391(10120):563–71.
- [13] Abbink P, et al. Protective efficacy of multiple vaccine platforms against Zika virus challenge in rhesus monkeys. *Science* 2016;353(6304):1129–32.
- [14] Pardi N, et al. Zika virus protection by a single low-dose nucleoside-modified mRNA vaccination. *Nature* 2017;543(7644):248–51.
- [15] Richner J, et al. Vaccine mediated protection against Zika virus induced congenital disease. *Cell* 2017;170:273–83.
- [16] Richner JM, et al. Modified mRNA vaccines protect against Zika virus infection. *Cell* 2017;168(6):1114–25 e10.
- [17] Dowd KA, et al. Rapid development of a DNA vaccine for Zika virus. *Science* 2016; 354(6309):237–40.
- [18] Larooca RA, et al. Vaccine protection against Zika virus from Brazil. *Nature* 2016; 536(7617):474–8.
- [19] Chattopadhyay A, et al. A recombinant virus vaccine that protects against both Chikungunya and Zika virus infections. *Vaccine* 2018;36(27):3894–900.
- [20] Gaudinski MR, et al. Safety, tolerability, and immunogenicity of two Zika virus DNA vaccine candidates in healthy adults: randomised, open-label, phase 1 clinical trials. *Lancet* 2018;391(10120):552–62.
- [21] Tebas P, et al. Safety and immunogenicity of an anti-Zika virus DNA vaccine - preliminary report. *N Engl J Med* 2017.
- [22] Shan C, et al. A live-attenuated Zika virus vaccine candidate induces sterilizing immunity in mouse models. *Nat Med* 2017;23(6):763–7.
- [23] Shan C, et al. A single-dose live-attenuated vaccine prevents Zika virus pregnancy transmission and testis damage. *Nat Commun* 2017;8(1):676.
- [24] Xie X, et al. Understanding Zika virus stability and developing a chimeric vaccine through functional analysis. *MBio* 2017;8(1).
- [25] Li XF, et al. Development of a chimeric Zika vaccine using a licensed live-attenuated flavivirus vaccine as backbone. *Nat Commun* 2018;9(1):673.
- [26] Ghaffarifar F. Plasmid DNA vaccines: where are we now? *Drugs Today (Barc)* 2018; 54(5):315–33.
- [27] Levine MM. "IDEAL" vaccines for resource poor settings. *Vaccine* 2011;29(Suppl. 4): D116–25.
- [28] Yang Y, et al. A cDNA clone-launched platform for high-yield production of inactivated Zika vaccine. *EBioMedicine* 2017;17:145–56.
- [29] Shan C, et al. An infectious cDNA clone of zika virus to study viral virulence, mosquito transmission, and antiviral inhibitors. *Cell Host Microbe* 2016;19(6): 891–900.
- [30] Xie X, et al. Zika virus replicons for drug discovery. *EBioMedicine* 2016;12:156–60.
- [31] Dupuy LC, et al. A DNA vaccine for Venezuelan equine encephalitis virus delivered by intramuscular electroporation elicits high levels of neutralizing antibodies in multiple animal models and provides protective immunity to mice and nonhuman primates. *Clin Vaccine Immunol* 2011;18(5):707–16.
- [32] Rossi SL, et al. Characterization of a novel murine model to study zika virus. *Am J Trop Med Hyg* 2016;94(6):1362–9.
- [33] Elong Ngonu A, et al. Mapping and role of the CD8(+) T cell response during primary zika virus infection in mice. *Cell Host Microbe* 2017;21(1):35–46.
- [34] Wild J, Hradecna Z, Szybalski W. Conditionally amplifiable BACs: switching from single-copy to high-copy vectors and genomic clones. *Genome Res* 2002;12(9): 1434–44.
- [35] Cheeseman HM, et al. Combined skin and muscle DNA priming provides enhanced humoral responses to an HIV-1 clade C envelope vaccine. *Hum Gene Ther* 2018.
- [36] Barzon L, et al. Infection dynamics in a traveller with persistent shedding of Zika virus RNA in semen for six months after returning from Haiti to Italy, January 2016. *Euro Surveill* 2016;21(32).
- [37] Nicastrì E, et al. Persistent detection of Zika virus RNA in semen for six months after symptom onset in a traveller returning from Haiti to Italy, February 2016. *Euro Surveill* 2016;21(32).
- [38] Russell K, et al. Male-to-female sexual transmission of zika virus-united states, January–April 2016. *Clin Infect Dis* 2017;64(2):211–3.
- [39] Minor PD. Live attenuated vaccines: Historical successes and current challenges. *Virology* 2015;479–480:379–92.
- [40] Hall RA, et al. DNA vaccine coding for the full-length infectious Kunjin virus RNA protects mice against the New York strain of West Nile virus. *Proc Natl Acad Sci U S A* 2003;100(18):10460–4.

- [41] Tretyakova I, et al. Plasmid DNA initiates replication of yellow fever vaccine in vitro and elicits virus-specific immune response in mice. *Virology* 2014;468-470:28–35.
- [42] Nickols B, et al. Plasmid DNA launches live-attenuated Japanese encephalitis virus and elicits virus-neutralizing antibodies in BALB/c mice. *Virology* 2017;512:66–73.
- [43] Tretyakova I, et al. DNA vaccine initiates replication of live attenuated chikungunya virus in vitro and elicits protective immune response in mice. *J Infect Dis* 2014; 209(12):1882–90.
- [44] Tretyakova I, et al. Novel vaccine against Venezuelan equine encephalitis combines advantages of DNA immunization and a live attenuated vaccine. *Vaccine* 2013; 31(7):1019–25.
- [45] Dupuis M, et al. Distribution of DNA vaccines determines their immunogenicity after intramuscular injection in mice. *J Immunol* 2000;165(5):2850–8.
- [46] Abbink P, et al. Durability and correlates of vaccine protection against Zika virus in rhesus monkeys. *Sci Transl Med* 2017(9):420.